Sea-surface CO2 fugacity in the subpolar North Atlantic

A. Olsen, K. R. Brown, M. Chierici, T. Johannessen, C. Neill

Biogeosciences, 5, 535–547, 2008
www.biogeosciences.net/5/535/2008/

Biogeosciences

Sea-surface CO_2 fugacity in the subpolar North Atlantic

A. Olsen[1,2,3], K. R. Brown[1], M. Chierici[3], T. Johannessen[2,1], and C. Neill[1]

[1]Bjerknes Centre for Climate Research, University of Bergen, Bergen, Norway
[2]Geophysical Institute, University of Bergen, Bergen, Norway
[3]Marine Chemistry, Department of Chemistry, Göteborg University, Göteborg, Sweden

Received: 25 April 2007 – Published in Biogeosciences Discuss.: 15 June 2007
Revised: 22 November 2007 – Accepted: 30 January 2008 – Published: 10 April 2008

Abstract. We present the first year-long subpolar trans-Atlantic set of surface seawater CO_2 fugacity (fCO_2^{sw}) data. The data were obtained aboard the MV *Nuka Arctica* in 2005 and provide a quasi-continuous picture of the fCO_2^{sw} variability between Denmark and Greenland. Complementary real-time high-resolution data of surface chlorophyll-*a* (chl-*a*) concentrations and mixed layer depth (MLD) estimates have been collocated with the fCO_2^{sw} data. Off-shelf fCO_2^{sw} data exhibit a pronounced seasonal cycle. In winter, surface waters are saturated to slightly supersaturated over a wide range of temperatures. Through spring and summer, fCO_2^{sw} decreases by approximately 60 μatm, due to biological carbon consumption, which is not fully counteracted by the fCO_2^{sw} increase due to summer warming. The changes are synchronous with changes in chl-*a* concentrations and MLD, both of which are exponentially correlated with fCO_2^{sw} in off-shelf regions.

1 Introduction

The rise in atmospheric CO_2 concentrations from man-made sources and resulting climate change is limited in part by oceanic carbon uptake. The annual ocean CO_2 uptake corresponds to roughly one quarter of annual emissions (Prentice et al., 2001). The extent to which ocean CO_2 uptake will be sustained in the future is an open question adding uncertainty to projections of climate change. Improved constraints on ocean CO_2 uptake in terms of large-scale, long-term changes will come from continuous measurements of ocean carbon cycle variables in key regions. The international ocean CO_2 research community has responded by developing a coordinated research effort to ensure collection of the required data in all ocean basins. These data include both snapshots of interior ocean carbon chemistry, like those collected during the WOCE/JGOFS global CO_2 survey (Wallace, 2001), and quasi-continuous observations of the surface-ocean CO_2 fugacity (fCO_2^{sw}) obtained through a variety of projects as recently summarised in the Surface Ocean CO_2 Variability and Vulnerability Workshop report (available at http://www.ioccp.org). The surface observations are mostly collected by autonomous instruments carried by a network of commercial vessels, Voluntary Observing Ships (VOS), and results have so far been presented on the annual surface-ocean carbon cycle in the North Pacific (Chierici et al., 2006), midlatitude North Atlantic (Lüger et al., 2004), subtropical North Atlantic (Cooper et al., 1998), and Caribbean Sea (Olsen et al., 2004; Wanninkhof et al., 2007). This paper presents the first set of fCO_2^{sw} data covering a full annual cycle obtained on the northernmost VOS line in the Atlantic Ocean, the MV *Nuka Arctica*, which crosses between Denmark and Greenland at approximately 60° N.

The North Atlantic is considered to be one of the more important CO_2 uptake regions of the world's oceans due to the extensive biological activity and cooling of waters travelling northward as the upper limb of the meridional overturning circulation. Indeed, data from the midlatitude regions show that surface waters are undersaturated throughout the year except in portions of the western basin where the waters are supersaturated in summer (Lüger et al., 2004). On the other hand, there is too little data from the high latitudes of the North Atlantic to describe a full annual cycle. As far as we are aware, the only published results are from the repeated visits from 1983 through 1991 to four stations located around Iceland (Takahashi et al., 1993) and the data from SURATLANT (Corbiere et al., 2007). However, both data sets originated from only the western regions of the northern North Atlantic and the SURATLANT data were calculated from shore-based analyses of total alkalinity (TA) and dissolved inorganic carbon (Ct), making the absolute values of

Correspondence to: A. Olsen
(are.olsen@gfi.uib.no)

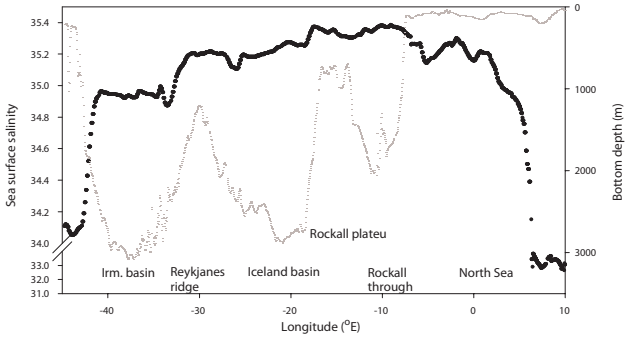

Fig. 1. FOAM SSS estimates (black) and bathymetry (grey) along a crossing that took place during 2–6 April 2005. The specific cruise track is shown in Fig. 2.

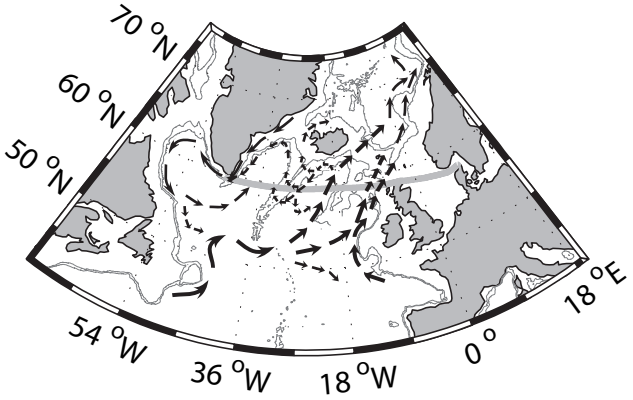

Fig. 2. Ship track from 2–6 April 2005 and main features of the surface circulation inspired by McCartney and Talley (1982), Hansen and Østerhus (2000), Frantantoni (2001), Orvik and Niiler (2002), and Reverdin et al. (2003). The scaling of the arrows is by no means exact. Isobaths have been drawn at the 1000 and 2000 m depth levels.

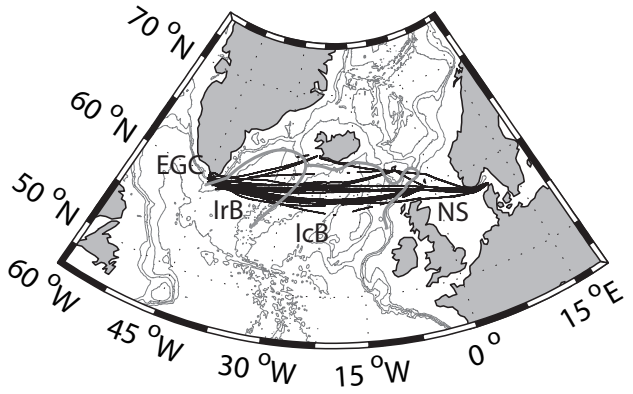

Fig. 3. *Nuka Arctica* fCO_2^{sw} sampling positions during 2005. Grey lines show isobaths at 500, 1500, 2500, and 3500 m. The heavy grey lines indicate approximately the boundaries of the regions introduced in Sect. 2.

fCO_2^{sw} less certain. For instance Wanninkhof et al. (1999) showed that fCO_2^{sw} determined from TA and Ct using different sets of carbonate dissociation constants can be biased by up to 20–40 μatm, and the random error in such values are between 5 and 10 μatm when compared to fCO_2^{sw} determined through infrared analysis.

Given the importance for the marine carbon cycle ascribed to the northern North Atlantic, a detailed description is overdue. This is provided here from data collected aboard *Nuka*. Because scientists are not allowed to travel aboard the *Nuka*, sampling for other biogeochemical parameters is limited. Thus, we took advantage of international remote sensing and data assimilation capabilities, using remotely sensed chlorophyll-*a* (chl-*a*) from the Sea-viewing Wide Field-of-view Sensor (SeaWiFS) that have been collocated with the *Nuka* fCO_2^{sw} data. We also present collocated sea surface salinity (SSS) and mixed layer depth (MLD) data from the Forecasting Ocean Assimilation Model (FOAM) of the U.K. National Centre for Ocean Forecasting (McCulloch et al., 2004).

2 Hydrographic setting

The hydrographic conditions along the track of *Nuka* are best illustrated through a section of sea surface salinity (SSS) and bathymetry as shown in Fig. 1. A map of the major surface currents is presented in Fig. 2. The North Sea is a shallow coastal ocean with a sharp salinity gradient at approximately 5° E. To the west, all waters are basically derivatives of the North Atlantic Current, NAC, frequently referred to as Sub-Polar Mode Water (SPMW) (McCartney and Talley, 1982). The SPMW circulates towards the west, progressively cooling and freshening and branching off to the Nordic Seas. The SPMW ends up in the Labrador Sea and mixes with waters of polar origin, forming Subarctic Intermediate Water (SAIW), which spreads east and north feeding back in on the SPMW, constituting a fresh and cold-end member for this water mass (Lacan and Jeandel, 2004; Pollard et al., 2004). Thus the most saline waters are found over the Rockall Trough and Plateau (Fig. 1) and these stem more or less directly from the NAC and the Continental Slope Current (CSC) (Hansen and Østerhus, 2000). Surface waters in the Iceland Basin (IcB), indicated in Fig. 3, are fresher and more homogenous as a result of local recirculation. The interior of the Irminger Basin (IrB) is dominated by SAIW, whereas the SPMW dominates waters overlying the rim of that basin as recognised in the slight peak in salinity over the East Greenland Shelf Edge. Far to the west is the East Greenland Current, carrying ice and low salinity waters from the Arctic Ocean southwards.

Since different processes may dominate in different areas, we have divided the sampling area into four regions (Fig. 3): (1) the East Greenland Current, (EGC), defined as the region between 45° W where sampling was terminated or initiated at each crossing and eastward to the 2750-m isobath; (2) the

IrB, which extends from the 2750-m isobath and eastward to the top of the Reykjanes Ridge, but excludes shelf areas around Iceland with a depth cut-off at 500 m; (3) the IcB region, covering the area between the top of the Reykjanes Ridge and eastward to the European continental shelf at the 500-m isobath (this region includes the Rockall Plateau but excludes shelf areas around Iceland and the Faeroes above 500 m); and (4) the region to the east of the 500 m isobath at the European continental shelf edge is the North Sea (NS).

3 Data

3.1 fCO_2^{sw} measurements

The container carrier MV *Nuka Arctica* is operated by Royal Arctic Lines of Denmark. The ship crosses the Atlantic at roughly 60° N in about five days, depending on the weather. Between the crossings, approximately one week is spent along the west coast of Greenland and three days in Aalborg, Denmark. The fCO_2^{sw} system was first installed on board during 2004. The data discussed here are from 2005, where collected data cover the full annual cycle. These data can now be obtained from the Carbon Dioxide Information Analysis Centre (CDIAC) at http://cdiac.esd.ornl.gov/oceans/home.html.

The fCO_2^{sw} instrument installed aboard *Nuka* analyzes the CO_2 concentration in an air headspace in equilibrium with a continuous stream of seawater using a LI-COR 6262 non-dispersive infrared (NDIR) CO_2/H_2O gas analyzer, and is a modified version of instruments described by Feely et al. (1998) and Wanninkhof and Thoning (1993). The main modifications are a smaller equilibrator and the method of drying the headspace air. Whereas the equilibrator in the referenced systems had a volume of 24 l, the equilibrator on *Nuka* has a volume of approximately 1.5 l. It is vented to the atmosphere via a smaller equilibrator to pre-equilibrate the vent air. The equilibrator headspace air is circulated at 70 ml min^{-1} through a Permapure Naphion dryer to the NDIR and then returned to the equilibrator. The NDIR is run in absolute mode. Equilibrator headspace samples are analysed every 2.5 min and the instrument is calibrated every 5th hour with three reference gases having approximate concentrations of 200 ppm, 350 ppm, and 430 ppm, which are traceable to reference standards provided by NOAA/Earth System Research Laboratory. The NDIR is zeroed and spanned once a day using a CO_2-free gas and the 430-ppm standard.

For our analysis the raw dry xCO_2 values reported by the NDIR were standardised using a linear fit between measured concentrations of the CO_2 standards and the offsets from calibrated values. Equilibrator CO_2 fugacity was calculated from the mole fraction as described by Feely et al. (1998) and Wanninkhof and Thoning (1993):

$$fCO_2^{eq} = xCO_2(p^{eq} - pH_2O)e^{p^{eq}\frac{B+2\delta}{RT_{eq}}} \quad (1)$$

where p^{eq} is the pressure of equilibration, pH_2O is the water vapour pressure (Weiss and Price, 1980), R is the gas constant, and B and δ are the first and cross virial coefficients (Weiss, 1974). Sea surface CO_2 fugacity, fCO_2^{sw}, was obtained by employing the thermodynamical fCO_2 temperature dependence of Takahashi et al. (1993) to correct for the roughly 0.5°C increase between intake and equilibrator temperatures.

In 2005, the instrument was installed in the bow and water was drawn from an intake at approximately 2 m depth. In bad weather, when the intake breached the surface, the instrument was shut down. Moreover, it was not possible to draw an air line from the bow down to the instrument for measurement of ambient marine air as is routinely done on such installations. Thus the atmospheric CO_2 data used here were obtained from the Climate Monitoring Division of NOAA/Earth System Research Laboratory (http://www.cmdl.noaa.gov/). Data of monthly mean mole fraction collected from Storhofdi, Vestmannaeyjar, Iceland (63.3° N) and Mace Head, Ireland (53.3° N) were linearly regressed to obtain the equations describing the latitudinal gradient of monthly mean xCO_2. From these equations, an atmospheric xCO_2 value was determined for each fCO_2^{sw} sample point. Mole fractions were converted to atmospheric CO_2 fugacity, fCO_2^{atm}, using Eq. (1) except that SST was used in place of T_{eq}.

In 2005, data were obtained on 27 of 30 crossings of the Atlantic, starting 7 January and ending 3 December when the ship went on a five-month charter in the Baltic. More than 46 000 measurements were obtained on the ship tracks shown in Fig. 3. The ship did a port call in Reykjavik on four occasions, hence the occurrence of a few more northerly routes.

3.2 Remotely sensed data

Surface-ocean chl-*a* data derived from radiation measurements of the SeaWiFS instrument carried aboard the SeaStar (ORBVIEW-2) spacecraft were obtained from the ocean color group at Goddard Space Flight Center at http://oceancolor.gsfc.nasa.gov (McClain et al., 2004). The SeaStar spacecraft was launched in 1997 and SeaWiFS data are available since September of that year. The Level-3 mapped eight day data product was used here. This is provided on a resolution of 1/12° in both latitude and longitude, which corresponds to 9.2 km in latitude and 4.6 km in longitude at 60° N. These approximately weekly averages were collocated with the fCO_2^{sw} data obtained on *Nuka* with a mean distance separation of 2.9 km spanning 0.04 to 5.2 km. The available chl-*a* data covered the time period 17 March to 23 October 2005. Following Lévy et al. (2005), chl-*a* values greater than 5 mg m^{-3} were considered unrealistically high and discarded, except for in the East Greenland Current region where much higher chl-*a* concentrations are known to

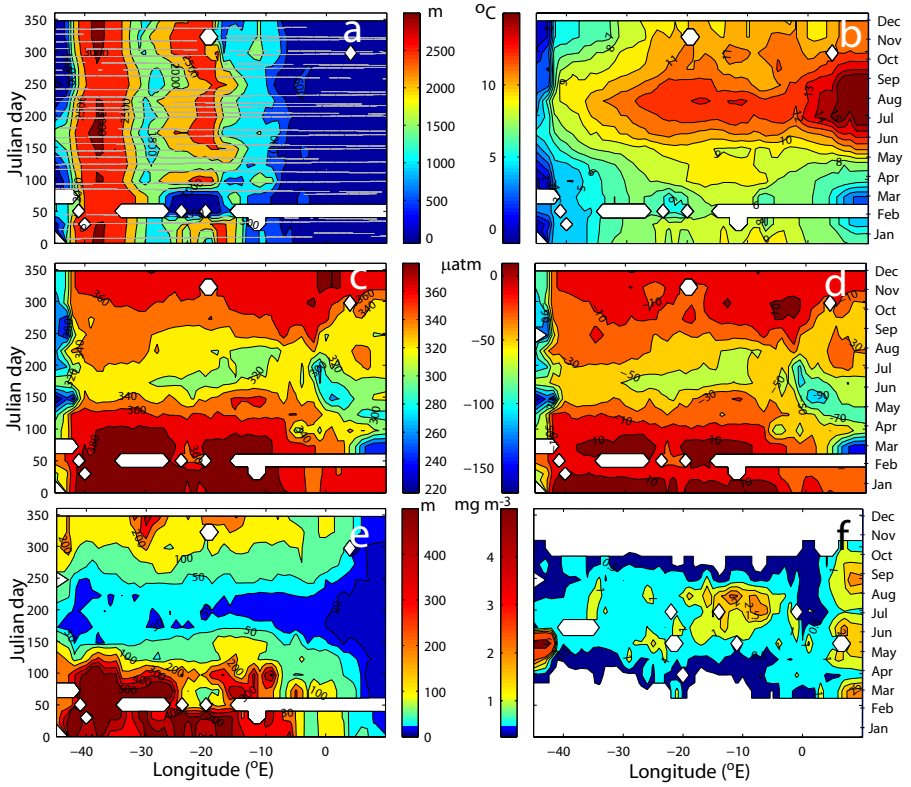

Fig. 4. Hovmöller diagrams of **(a)** *Nuka* ship tracks (grey) and bathymetry, **(b)** SST, **(c)** fCO_2^{sw}, **(d)** ΔfCO_2 (negative values reflect undersaturation), **(e)** MLD, and **(f)** chl-*a* along the track of *Nuka* in 2005. For chl-*a*, isolines have been drawn only for concentrations up to 5 mg m^{-3}. The gridding was carried out by bin-averaging the data into cells of size 1° and 20 days. Grid cells that lack data are left blank.

occur (Holliday et al., 2006). This removed 193 of 21 806 collocated chl-*a* observations.

3.3 Ocean analysis data

The SSS and MLD estimates for 2005 along the track of *Nuka* supplied by FOAM can be obtained at http://www.ncof.gov.uk/products.html (McCulloch et al., 2004). These data are provided as daily fields on a 1/9° resolution, corresponding to 12.3 km in latitude and 6.2 km in longitude at 60° N. The ocean data assimilated by FOAM are obtained from a number of sources such as Argo profiling floats, XBT and CTD profiles, and AVHRR satellite-derived sea surface temperatures. MLD in FOAM is determined as the depth where a density difference of 0.05 kg m^{-3} from the surface value occurs (Chunlei Liu, Environmental Systems Science Centre of the U.K. National Environmental Research Council, personal communication). The daily FOAM data were collocated with the *Nuka* fCO_2^{sw} data with a distance separation of between 0 and 7.8 km, with a mean value of 4 km.

To evaluate of the reliability of the FOAM data, FOAM SST estimates were compared with the temperatures measured at the seawater intake on *Nuka*. Linear regression (not shown) gave an r^2 value 0.92 and a root mean square (rms) error 0.82. No bias at any particular SSTs could be identified. The FOAM SSS data were also compared to the SSS data that were collected by the thermosalinograph (TSG) aboard *Nuka*. In 2005, the TSG on *Nuka* collected data on 12 of the 27 crossings with fCO_2^{sw} data; FOAM data were preferred to get a complete dataset. Regression between FOAM SSS and TSG SSS gave a r^2 value of 0.88 and a rms of 0.27 (not shown).

4 Results

Hovmöller diagrams of SST, fCO_2^{sw}, ΔfCO_2, MLD, and chl-*a* are shown in Fig. 4. In addition Panel 4a shows ship tracks and bathymetry to illustrate when variations of the ship track may have affected the results. In particular, there were the atypical values of SST (Fig. 4b), fCO_2^{sw} (Fig. 4c), ΔfCO_2 (Fig. 4d), and MLD (Fig. 4e) encountered at 20° W in February on the Iceland Shelf (Fig. 4a) when the ship was on its way to a port call in Reykjavik.

All variables except SSS (not shown) went through a pronounced seasonal cycle in 2005. The highest fCO_2^{sw} values, lowest SSTs, and deepest MLDs were encountered from January through March. Waters over both the IcB and IrB were

slightly supersaturated with respect to the atmospheric fCO_2 level, and the NS and EGC were slightly undersaturated. During this period, the warmest waters occurred over the IcB and were between 8 and 9°C. To the east, within the NS, temperatures dropped to around 6°C; to the west, within the IrB and into the EGC, temperatures decreased from around 7°C to less than 1°C.

In April 2005, the water began to warm and continued to do so until September. At that time, temperatures in the eastern NS had reached above 15°C, those in the IcB were between 12 and 13°C, and those in the IrB were between 6 and 11°C depending on longitude. In the EGC, the warming was less pronounced.

This warming stratified the water column (Fig. 4e), which initiated a phytoplankton bloom (Fig. 4f) drawing down the fCO_2^{sw} (Fig. 4c and d). We quantify the relative importance of specific fCO_2^{sw} drivers in Sect. 5.1. The seasonal evolution in fCO_2^{sw} is synchronous with that for the MLD and for chl-*a*. In the IrB, the MLD shoaled from several hundred meters to 50 m by June–August. In this period, surface chl-*a* values were normally between 0.5 and 1 mg m^{-3} and the fCO_2^{sw} levels had decreased to between 320 and 340 μatm. The fCO_2^{sw} drawdown was larger in the IcB, where values were less than 320 μatm; this appears coherent with the higher chl-*a* concentrations and shallower MLD that occurred here compared to the IrB. As evaluated from the fCO_2^{sw} values, the bloom in the IcB appears to have progressed eastward with minimum values occurring at about 20° W in late June, and then at about 10° W in late July and early August. A similar pattern is evident in the chl-*a* and MLD data: peak chl-*a* concentrations were reached earlier toward the Reykjanes Ridge than toward the Rockall Trough, and the MLD was shallower to the west in early summer and to the east in late summer. The specific correlations of fCO_2^{sw} versus chl-*a* and MLD are further explored in Sects. 5.2.2 and 5.2.3, respectively.

In the EGC, it appears as if the bloom peaked in May, with chl-*a* concentrations exceeding 5 mg m^{-3} and fCO_2^{sw} values having decreased to less than 300 μatm, but this is uncertain as the succeeding ship tracks took a more southern route and data collection was stopped before the ship entered the shelf (see Fig. 4a). This is most likely the reason for the increase in fCO_2^{sw} that appears to have occurred in June before low values were re-encountered in August and September.

In the NS, the seasonal cycle in chl-*a* is not as clear as in the other regions. In the western regions of the NS, concentrations were between 0.5 and 1 mg m^{-3} throughout the year. In the eastern regions of the NS, chl-*a* concentrations appear to have peaked twice, once in May–June and again in August–September. None of these features appear particularly coherent with the fCO_2^{sw} variability, which indicates that the bloom progressed from east to west between April and July.

By September, the mixed layer started to deepen and surface waters became colder. No chl-*a* data were available after late October, and by that time the concentration had dropped to between 0.25 and 0.5 mg m^{-3} and fCO_2^{sw} had increased to approximately 360 μatm. By December when data collection aboard *Nuka* ended for the year, fCO_2^{sw} was close to saturation with respect to the atmospheric concentration.

5 Discussion

The data collected on *Nuka* give a clear view of the seasonal fCO_2^{sw} variability across the subpolar North Atlantic. The summertime drawdown of around 60 μatm in the IrB and IcB is less than the drawdowns observed by Takahashi et al. (1993) of ~140 μatm at their western station (64.5° N, 28 ° W) and ~100 μatm at their southern station (63° N, 22° W). It is also less than the seasonal amplitude of ~100 μatm in the climatological data of Takahashi et al. (2002), but similar to the 60 μatm amplitude modelled for 60° N by Taylor et al. (1991).

In winter, the ocean was saturated to slightly supersaturated with respect to the atmospheric concentrations, except for in the EGC and NS, which were undersaturated. This is in accordance with Takahashi et al. (1993) who also observed saturated-to-supersaturated waters at their southern station during winter. In contrast, both Olsen et al. (2003) and Takahashi et al. (2002) estimated substantial undersaturation during winter over the whole region covered by *Nuka*. Specifically, Olsen et al. (2003) determined an undersaturation of between 10 and 15 μatm as evaluated from their Figs. 4a and 7, whereas according to Takahashi et al. (2002) the mean undersaturation during January–March is 16±18 μatm (mean $\pm\sigma$) between 40° W and the Greenwich meridian (as determined from data obtained at http://www.ldeo.columbia.edu/res/pi/CO2/). To improve this situation, the 2005 *Nuka* data are now included in the next climatology of Takahashi et al. (2007[1]).

As for winter values, our observations support the conclusion of Perez et al. (2002), who found that the air-sea disequilibrium in total dissolved inorganic carbon in this region must be quite small during the time of water mass formation, which is winter. In contrast, the disequilibrium estimates of Gruber et al. (1996) showed undersaturation of more than 30 μatm in winter in the region.

The remainder of the discussion focuses on seasonal fCO_2^{sw} variations. In particular, we analyse what processes control variations (Sect. 5.1) and explore the relationships between fCO_2^{sw} and other environmental parameters related to these processes, with emphasis on identifying suitable fCO_2^{sw} extrapolation parameters (Sect. 5.2).

[1]Takahashi, T., Sutherland, S., Wanninkhof, R. et al.: Climatological Mean and Decadal Change in Surface Ocean pCO_2 and Net Sea-Air Flux over the Global Oceans, Deep-Sea Res., submitted, 2007.

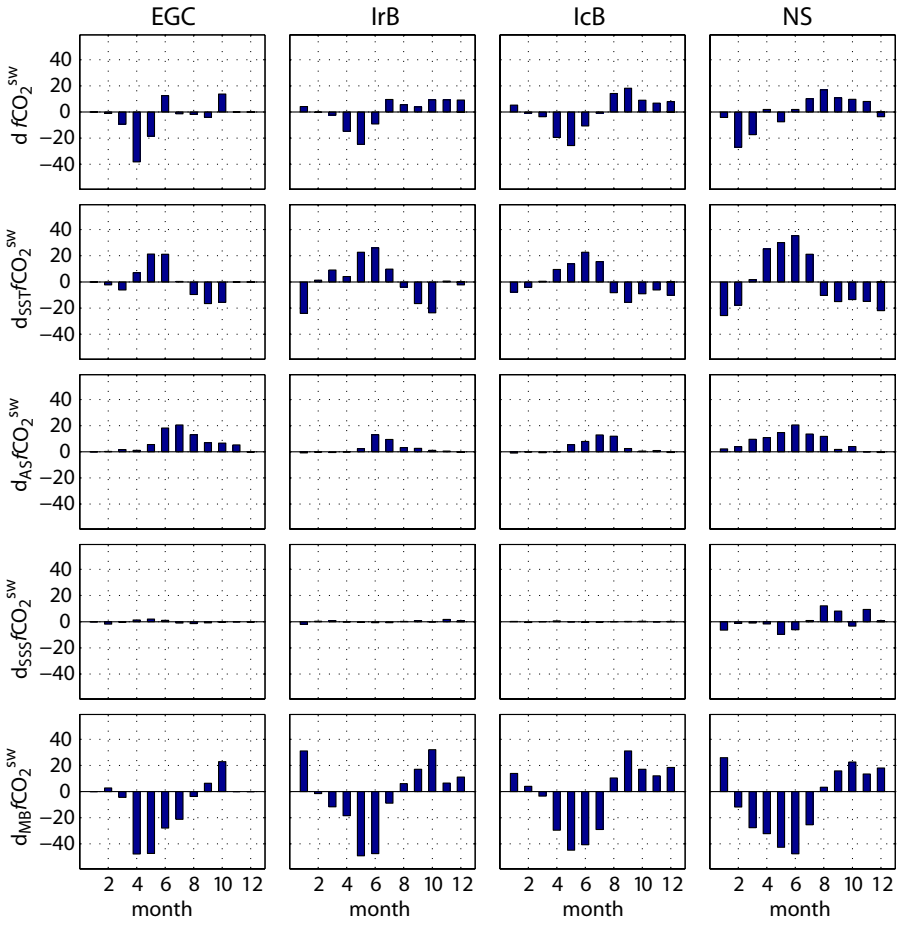

Fig. 5. The upper row shows the observed changes in fCO_2^{sw} (in μatm) in the EGC, IrB, IcB, and NS for each month. The second to fourth rows show the corresponding expected changes in fCO_2^{sw} due to observed changes in temperature, air-sea gas exchange, and salinity each month, while the fifth row shows changes in fCO_2^{sw} due to biology plus mixing. Negative values reflect a decrease in fCO_2^{sw}.

5.1 Analysis of factors controlling monthly changes of fCO_2^{sw}

The seasonal variations seen in the *Nuka* fCO_2^{sw} data are the combined result of multiple processes, which affect surface-ocean carbon. The large decrease in fCO_2^{sw} despite substantial warming during spring indicates that biology is the dominant driver. Here we determine the specific variations in fCO_2^{sw} brought about by variations in temperature, air-sea gas exchange, salinity variations, and mixing and biology.

Temperature affects fCO_2^{sw} thermodynamically, which is determined following the relationship established by Takahashi et al. (1993). Air-sea gas exchange affects fCO_2^{sw} because it alters Ct but not TA. It is determined through multiplying the air-sea disequilibrium with a gas transfer coefficient. Salinity affects fCO_2^{sw} through concentration or dilution of TA and Ct, and through changes in the CO_2 solubility and carbonic acid dissociation constants (Takahashi et al., 1993). This has been shown to have a significant impact on seasonal fCO_2^{sw} variations in the Caribbean Sea (Wanninkhof et al., 2007). The effect was determined by linearly adjusting TA and Ct for salinity changes and recomputing fCO_2^{sw} using thermodynamic carbon system equations. Finally, mixing and biology affect fCO_2^{sw} through Ct, an effect that can be determined from changes in nutrient concentrations as did Lüger et al. (2004) and Chierici et al. (2006). However, we could not use this approach for this study because no nutrient data were obtained onboard the *Nuka* in 2005. Instead, we evaluate this mixing+biology effect as the monthly change in fCO_2^{sw} that is left unexplained by the other processes mentioned previously. Thus we have

$$d\,fCO_2^{sw} = d_{SST}\,fCO_2^{sw} + d_{AS}\,fCO_2^{sw} + d_{SSS}\,fCO_2^{sw} + d_{MB}\,fCO_2^{sw} \quad (2)$$

The left hand term is the observed monthly change in fCO_2^{sw}, the first term on the right hand side is the change due to SST changes, the second right-hand term is the change due to air-sea gas exchange, and the third and fourth right-hand terms are the changes due to salinity variations and mixing plus biology, respectively. The specific details as to how each

term is computed and the associated error analyses are provided in the appendix.

The results of these calculations are displayed in Fig. 5, where positive values indicate an increase in fCO_2^{sw}. The most dramatic changes in fCO_2^{sw} in 2005 occurred in the EGC in April when it decreased by almost 40 μatm. The monthly changes in the IrB and IcB were not as large and came later, reaching nearly 30 μatm in May 2005. In the NS, the largest drawdown occurred in February, almost 30 μatm. In this region, the fCO_2^{sw} was less variable from April through June 2005, but showed a steady increase from July to November. In the IcB, increasing values occurred one month later, in August, whereas the increase started in July in the IrB. As mentioned in Sect. 4, we consider that the fCO_2^{sw} increase in June in the EGC is an artefact due to a southward shift in the ship track. Thus in this region, the autumn increase appears to have set in as late as October. It is also evident that the observed changes in fCO_2^{sw} in both the IrB and IcB follow those expected from mixing and biology, while the effects of temperature and gas exchange play a smaller role, as was also modelled by Taylor et al. (1991). This result also agrees with that of Takahashi et al. (2002) for the effect of seasonal temperature changes and biology (their Fig. 9). Gas exchange is only important in summer and early fall when the air-sea CO_2 gradient is large and mixed layers are shallow. Changes in SSS do not have a substantial effect on fCO_2^{sw} in any region except for the NS. There it seems to have induced decreases in fCO_2^{sw} during May and June. This may have resulted from a decrease in salinity due to increased runoff. Also, the salinities of inflowing Atlantic water are typically higher in winter than in summer (Lee et al., 1980). However, given the large spatial salinity gradients in the NS (Fig. 1 and Lee et al., 1980), the effect can just as well be due to changes in the ship track. The air-sea flux had a larger effect on fCO_2^{sw} in the NS and EGC than in the IrB and IcB, because of larger air-sea gradients and shallower mixed layers (Fig. 4). During the first half of the year, fCO_2^{sw} in the NS is affected at least as much by temperature as by biology plus mixing.

In the EGC, biology plus mixing appears to have dominated fCO_2^{sw} variations from February through May. During the rest of the year there is no dominant process, although salinity-induced changes are negligible.

5.2 Relationship between fCO_2^{sw} and environmental parameters

One of the ultimate goals of the global fCO_2^{sw} observation effort is to constrain regional ocean carbon uptake on seasonal-to-interannual timescales. To achieve this task through ocean observations alone would require substantial investments of both time and money. Moreover, instrument failure and availability of ships will inevitably restrict sampling coverage. This situation could be improved by extrapolating fCO_2^{sw} fields from data provided by space-borne sensors having near synoptic global coverage, the feasibility of which has been demonstrated using SST in regions like the North Pacific (Stephens et al., 1995), Equatorial Pacific (Boutin et al., 1999; Cosca et al., 2003), and Sargasso and Caribbean Seas (Nelson et al., 2001; Olsen et al., 2004). However, in the higher latitudes of the North Atlantic, SST is less useful, particularly in summer (Olsen et al., 2003), most likely due to the strong biological component of fCO_2^{sw} variations as discussed in the previous section. Other variables such as chl-*a* have been suggested, but recent findings reveal that there is either no correlation (Lüger et al., 2004; Nakaoa et al., 2006) or else only some correlation over short distances (Watson et al., 1991).

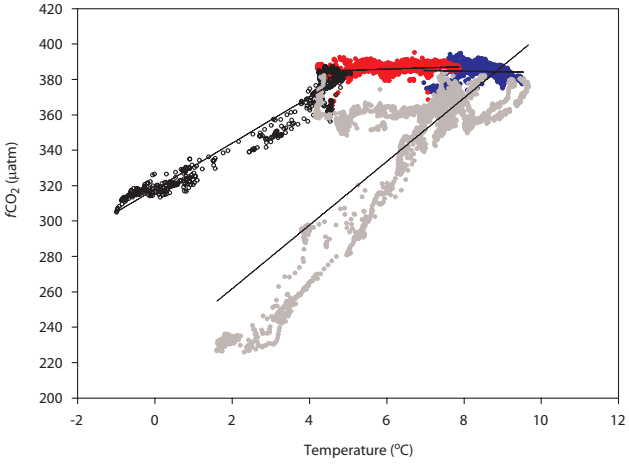

Fig. 6. Relationship between fCO_2^{sw} and SST during winter (January–March) in the EGC (open), IrB (red), IcB (blue), and NS (grey). The black lines show the linear regressions for each region.

We use the *Nuka* data, with their high frequency and annual coverage, as an opportunity to track down relationships that may exist in the subpolar North Atlantic. We explore the individual relationships of fCO_2^{sw} versus SST, chl-*a*, and MLD, all of which showed an apparent covariation with fCO_2^{sw} in Fig. 4. Multiple regression and flux calculations are the focus of Chierici et al. (2007)[2].

5.2.1 Relationship with temperature

Figure 6 presents wintertime (January–March) fCO_2^{sw} plotted as a function of SST in each of the regions introduced in Section 2. Regression diagnostics of the linear fits drawn in Fig. 6 are listed in Table 1, along with the number of observations and fCO_2^{sw} standard deviations for comparison with the rms values. The wintertime, off-shelf fCO_2^{sw} in the subpolar North Atlantic is not related to temperature as evalu-

[2]Chierici, M., Olsen, A., Triñanes, J., Johannessen, T., and Wanninkhof, R.: Algorithms to estimate the carbon dioxide uptake in the northern North Atlantic using ship observations, satellite and ocean analysis data, Deep-Sea Res., submitted, 2007.

Table 1. Regression diagnostics for the relationship fCO_2^{sw}=a∗SST+b in the different regions during winter (January–March.).

Region	a	b	r^2	rms	stdev. in data	n
IcB	−0.373	387.64	0.0024	3.90	3.91	2388
IrB	0.694	381.67	0.0080	2.47	2.58	1906
EGC	13.0	317.98	0.96	5.65	27.3	670
NS	18.0	225.81	0.67	22.2	38.4	3042

ated from the *Nuka* 2005 data. In both the IcB and IrB, the wintertime fCO_2^{sw} remained near 385 μatm (mean values of 384 and 386 μatm, respectively) over SSTs ranging from 4 to above 8°C. At temperatures higher than 8.5°C, there is a slight tendency for fCO_2^{sw} to decrease with increasing temperatures.

In the EGC, wintertime fCO_2^{sw} follows approximately the thermodynamic relationship of Takahashi et al. (1993), increasing by 3.8% $°C^{-1}$ over the range of temperatures of −1 to 4.5°C. This relationship is quite strong and explains 96% of the variability in fCO_2^{sw} . In the NS several temperature dependant relationships seem to exist in winter. The data that define the most obvious relationship were acquired in March, and the positions of these encompass the other data on the plot that were obtained in January and February. Thus the different slopes may reflect seasonal changes in the slope.

Throughout the rest of the year fCO_2^{sw} is poorly related to temperature. Linear regression using data from the whole year (not shown) gave r^2 values of 0.2 for the EGC, 0.01 for the NS, and 0.56 and 0.50 for the IcB and IrB, respectively. In the two latter regions, the slopes of the relationships were negative, reflecting the dominating impact of mixing plus biology on annual fCO_2^{sw} variations (see Sect. 5.1). Additionally, for any given temperature, fCO_2^{sw} was around 30–40 μatm higher in fall than in spring. This causes a substantial variation in the annual fCO_2^{sw}-SST relationships. We believe that this is mainly a result of the uptake of CO_2 from the atmosphere over summer, which accumulates, increasing fCO_2^{sw} by about 40 μatm in these regions (Fig. 5, row 4).

5.2.2 Relationship with chlorophyll-*a*

As with Lüger et al. (2004) and Nakaoa et al. (2006), linear relationships between fCO_2^{sw} and chl-*a* could not be identified on an annual scale in any of the regions that we have defined, but that does not mean that there is no relationship on smaller spatial and temporal scales, as shown by Watson et al. (1991). However, in the IrB and IcB we find an exponential relationship between chl-*a* and fCO_2^{sw} (Fig. 7a, Table 2) for data from March through October, the time period for which SeaWiFS chl-*a* data were available. It is not surprising that a relationship exists during spring when primary production reduces fCO_2^{sw} (see Sect. 5.1). On the other hand, after the bloom one would expect a rapid decline of chl-*a* as nutrients become exhausted, but a slow increase of fCO_2^{sw} owing to mixing of deep, high CO_2 waters into the surface layer. However, our data suggest that high chl-*a* levels are to a large extent maintained throughout summer when the fCO_2^{sw} is low, as is evident with the exponential shape of the fCO_2^{sw}-chl-*a* relationship. Possibly, this reflects primary production from regenerated rather than new nutrients.

There is some variation in the accuracy of the chl-*a* relationships with season. As illustrated in Fig. 8a, the chl-*a* relationships do not fully reproduce the seasonal amplitude in fCO_2^{sw} and tend to underestimate high fCO_2^{sw} values and overestimate low ones. This tendency appears stronger in the IcB than in the IrB. In the EGC and NS regions, there is little relationship between fCO_2^{sw} and chl-*a* (Table 2 and Fig. 7b).

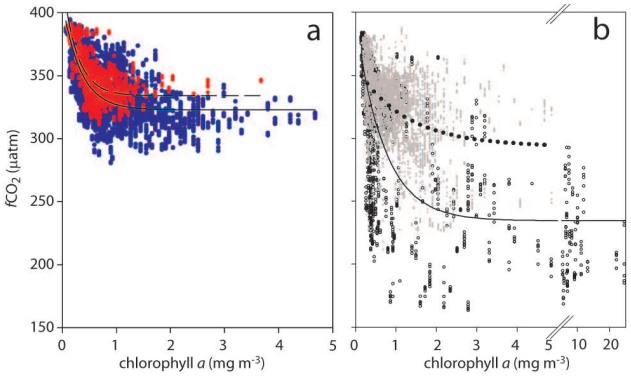

Fig. 7. Relationship between fCO_2^{sw} and chl-*a* in **(a)** the IcB (blue) and IrB (red) and **(b)** in the EGC (open) and in the NS (grey) during March-October. In (b) there is a break at 5 mg m^{-3} in the chl-*a* axis. In (a), the solid and dashed lines show the exponential regressions in the IcB and IrB, respectively. In (b), exponential regressions are shown for the: EGC (solid) and the NS (dotted).

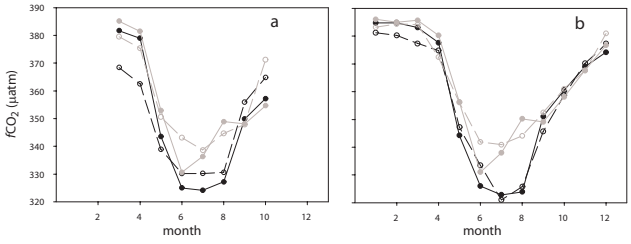

Fig. 8. Monthly mean observed (solid lines with solid circles) and predicted (dashed lines with open circles) fCO_2^{sw} in the IcB (black) and IrB (grey). In panel **(a)**, fCO_2^{sw} was computed using the chl-*a* dependencies (Table 2); in **(b)**, it was computed using the MLD dependencies (Table 3). Only data with collocated SeaWiFS chl-*a* observations were used to create the curves in (a), similarly, for (b) only data with collocated FOAM MLD estimates were used. This explains the slight differences between the observed data curves in (a) versus (b).

Table 2. Diagnostics for the equation $fCO_2^{sw}=a+b*e^{-c(\text{chl-}a)}$ for the different regions from March–October.

Region	a	b	c	r^2	rms	stdev. in data	n
IcB	322.92	84.92	3.01	0.52	15.6	22.4	7295
IrB	334.13	91.54	3.77	0.70	10.4	19.1	3917
EGC	234.47	160.3	1.43	0.49	40.6	56.6	2283
NS	293.45	63.36	0.81	0.21	24.4	27.4	7191

5.2.3 Relationship with mixed layer depth

Subpolar North Atlantic fCO_2^{sw} values are related to MLD through exponential growth curves as illustrated in Fig. 9a and summarised in Table 3. This relationship is not surprising given that seasonal fCO_2^{sw} variations are largely controlled by mixing and biology (see Sect. 5.1). Primary production, which reduces fCO_2^{sw}, starts with the formation of a shallow mixed layer (Sverdrup, 1953) and mixing during fall brings deep, nutrient-rich, high-CO_2 water to the surface. The shape of the relationship suggests a linear relationship between fCO_2^{sw} and MLD from the beginning of the bloom until the MLD deepens during fall, and reflects the stabilisation of fCO_2^{sw} near saturation levels in winter.

As illustrated in Fig. 8b, the MLD relationships reproduce the seasonal amplitude in fCO_2^{sw} better than the chl-*a* relationships. In the IrB, no particular bias appears in any of the seasons. In the IcB there is a negative bias of approximately 5 μatm in winter; otherwise the estimates are accurate. In the IcB, the fCO_2^{sw}-MLD relationship explains 81% of the variability in fCO_2^{sw}; in the IrB, 77%. On its own, MLD can reproduce fCO_2^{sw} to better than $\pm 10\,\mu$atm in the IrB and $\pm 12\,\mu$atm in the IcB on an annual basis. This is approximately the accuracy required to estimate the northern North Atlantic annual sink size to within 0.1 Gt yr^{-1} (Sweeney et al., 2002).

On the shelves, MLD regressions are not as good (Fig. 9b), in particular in the EGC where an exponential growth curve fails to reproduce fCO_2^{sw} variability. In the NS, the relationship with MLD is better than the relationship with chl-*a*, but it can only estimate fCO_2^{sw} to within $\pm 26\,\mu$atm.

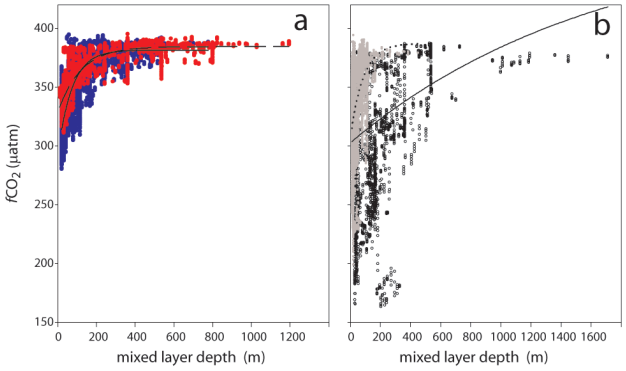

Fig. 9. Annual relationships between fCO_2^{sw} and MLD in **(a)** the IcB (blue) and IrB (red) and **(b)** the EGC (open) and the NS (grey). In (a), the solid and dashed lines show exponential regressions in the IcB and IrB, respectively. In (b), exponential regressions are shown for the: EGC (solid) and NS (dotted).

6 Conclusions

The data collected aboard *Nuka Arctica* in 2005 have given an unprecedented view of annual surface ocean fCO_2 variability in the subpolar North Atlantic. Excluding shelf areas, the fCO_2^{sw} was essentially in equilibrium with the atmospheric concentration in winter. Throughout summer it was reduced by approximately 60 μatm, the net result of a biological drawdown of CO_2 that was not fully counteracted by the increase in temperature and uptake of CO_2 from the atmosphere. In fall the dominating processes were mixing plus biology and gas exchange, which resulted in an fCO_2^{sw} increase.

The relationship between fCO_2^{sw} and three potential extrapolation parameters were investigated. Our analyses showed that during winter, fCO_2^{sw} is related to SST in the EGC. In the NS, several relationships appear to exist in this season. In the IcB and IrB, wintertime fCO_2^{sw} is almost constant at near saturation levels over a wide range of temperatures. On an annual basis, however, the correlation between SST and fCO_2^{sw} is poor in the shelf regions, with an r^2 of 0.2 in the ECG and 0.01 in the NS. In the IcB and IrB the annual correlation coefficients are better (0.56 and 0.50, respectively) but still leave much variability unexplained. Therefore it is not appropriate to use SST as a stand alone fCO_2^{sw} annual regression variable in the northern North Atlantic, as done for instance by Nakaoa et al. (2006) and Park et al. (2006).

We have been able to identify basin-wide relationships between fCO_2^{sw} and chl-*a*, valid from mid-March to mid-October when chl-*a* data were available. An exponential decay curve describes the relationship with a rms of 15.6 μatm in the IcB and 10.4 μatm in the IrB. We believe that the shape of the curve reflects the fact that new production is limited by nutrient availability during summer. Similar curves should be tested in other regions as well.

Table 3. Diagnostics for the equation $fCO_2^{sw}=a-b*e^{-c\mathrm{MLD}}$ for the different regions using data from throughout the year.

Region	a	b	c	r^2	rms	stdev. in data	n
IcB	381.54	88.84	0.014	0.81	11.3	25.6	16693
IrB	384.60	56.26	0.0086	0.77	9.45	19.6	9007
EGC	482.58	179.89	0.00060	0.12	48.2	51.3	3974
NS	387.42	81.30	0.012	0.32	26.0	31.5	13952

The relationship between fCO_2^{sw} and MLD was strong in the IrB and IcB. Given the dependence of fCO_2^{sw} on biology plus mixing as shown in Sect. 5.1, as well as the reliance of biology on mixing (Sverdrup, 1953), this relationship is not unexpected. The relationship followed approximately an exponential growth curve, the combination of a linear relationship during spring, summer and fall, and fCO_2^{sw} being constant as MLD exceeded 300 m, typical during winter. By itself the MLD relationship reproduced fCO_2^{sw} to within $\pm 10\,\mu$atm in the IrB and $\pm 12\,\mu$atm in the IcB.

In order to quantify the North Atlantic CO_2 sink size to within $0.1\,\mathrm{Gt\,yr^{-1}}$, fCO_2^{sw} would need to be mapped with an accuracy of $10\,\mu$atm (Sweeney et al., 2002). Not considering the fCO_2^{sw} measurement accuracy of $2\,\mu$atm (Pierrot et al., 2007[3]) this seems to be within reach given the relationships identified in the present study. This has been further explored by Chierici et al. (2007)[2]. Using fCO_2^{sw} data from *Nuka* they found that between 10° W and 40° W, the combination of SST, chl-*a*, and MLD as regression variables allows fCO_2^{sw} to be reproduced with an accuracy of $10\,\mu$atm throughout the year, as validated with independent fCO_2^{sw} data.

In the NS and EGC, annual regressions were generally not as good as in the IcB and IrB, which may reflect seasonal changes in slopes, insufficient data coverage, and more heterogeneous hydrographic conditions. It is also possible, given local heterogeneity, that FOAM performs poorly in these regions. More dedicated studies should investigate these regions.

Appendix A

This appendix details how we computed each term on the right side of Eq. (2), as well as associated errors.

X^i indicate the monthly mean of parameter X in question. Additionally, since we are interested in changes occurring during each month, estimates of parameter values for the first of each month are required. These are denoted as $X^{i,1}$ and computed as

$$X^{i,1} = \frac{X^{i-1} + X^i}{2} \tag{A1}$$

The total monthly change in fCO_2^{sw} was computed as

$$d\,fCO_2{}^{sw,i} = fCO_2{}^{sw,i+1,1} - fCO_2{}^{sw,i,1} \tag{A2}$$

The change in fCO_2^{sw} induced by the change in temperature during each month i was computed as

$$d_{SST}\,fCO_2{}^{sw,i} = fCO_2{}^{sw,i,1} e^{0.0423(SST^{i+1,1}-SST^{i,1})} - fCO_2{}^{sw,i,1} \tag{A3}$$

The change due to air-sea gas exchange was computed as

$$d_{AS}\,fCO_2{}^{sw,i} = f(Ct^{i,1} + dCt_{AS}{}^i, TA^{i,1}, SSS^{i,1}, SST^{i,1}) - f\left(Ct^{i,1}, TA^{i,1}, SSS^{i,1}, SST^{i,1}\right) \tag{A4}$$

where the function is the system of equations relating the inorganic species. All CO_2 system calculations were carried out using constants of Merbach et al. (1973) refit by Leuker et al. (2000) and the Matlab code provided by Zeebe and Wolf-Gladrow (2001), but modified to work with CO_2 fugacity rather than partial pressure. The effects of phosphate and silicate were ignored, this may correspond to an error of up to $2\,\mu$atm and is negligible for the present purposes. For the IrB and IcB regions, TA was estimated using the function derived by Lee et al. (2006), for the EGC we used the equation of Bellerby et al. (2005). For the NS we used the function TA=21.533S+1610, derived from data obtained on the 64PE184, 64PE187, 64PE190 and 64PE195 cruises (A. Omar, personal communication). Ct values were determined from $fCO_2{}^{sw,i}$ and estimated TA. The air-sea gas exchange contribution was determined as

$$dCt_{AS}{}^i = \frac{d^i \times F^i}{MLD^i} \tag{A5}$$

where d^i is the number of days each month and F^i is the mean flux each month according to

$$F^i = S^i k^i \left(fCO_2{}^{atm,i} - fCO_2{}^{sw,i}\right) \tag{A6}$$

[3]Pierrot, D., Neill, C., Sullivan, K. et al.: Recommendations for autonomous underway pCO_2 measuring systems and data reduction routines, Deep-Sea Res., submitted, 2007.

where S^i is the monthly mean solubility computed following Weiss (1974). The mean transfer velocity each month, k^i, was determined following Wanninkhof (1992):

$$k^i = 0.31 \times \left(\frac{\sum_{j=1}^{n} U_{10,j}^2}{n} \right)^i \left(\frac{Sc^i}{660} \right)^{-\frac{1}{2}} \quad \text{(A7)}$$

where $U_{10,j}$ is 6 hourly wind speed data and n is the number of data in each region in each month i. The wind speeds were computed from the 6 hourly orthogonal velocity components at 10 m provided in the NCEP/NCAR reanalysis product (Kalnay et al., 1992).

Finally, the effect of salinity changes on fCO_2 was determined as

$$d_{SSS} fCO_2{}^{sw,i} = f(Ct^{i,1}, TA^{i,1}, SSS^{i,1}, SST^{i,1}) - f\left(Ct^{i,1} \frac{sss^{i+1,1}}{sss^{i,1}}, TA^{i,1} \frac{sss^{i+1,1}}{sss^{i,1}}, SSS^{i+1,1}, SST^{i,1} \right) \quad \text{(A8)}$$

Despite some uncertainties, these results appear robust, as discussed below. One source of uncertainty in the calculations is the use of TA and Ct estimates in Eqs. (A4) and (A8). However, adjustments of the TA estimates by as much as $\pm 200\,\mu mol\,kg^{-1}$ resulted in changes of the $d_x\ fCO_2^{sw}$ values of up to only a few μatm. Similarly, changing the set of constants used in the CO_2 system calculations to those of Roy et al. (1993), which gives fCO_2^{sw} values most offset from those calculated using the Mehrbach et al. (1973) constants (Wanninkhof et al., 1999), resulted in changes in $d_x\ fCO_2^{sw}$ of less than 1 μatm. The reason for this small effect is that the $d_x\ fCO_2^{sw}$ values are determined by difference, so systematic errors in the TA estimates and carbon system parameters cancel out.

The other major source of uncertainty is the gas transfer velocity estimate, in terms of both the $k-U_{10}$ parameterisation and wind speed data. Changing the $k-U_{10}$ parameterisation to that of Wanninkhof and McGillis (1999) had a minor effect on the $d_{AS}\ fCO_2^{sw}$ estimates. The magnitude and direction of the shift depended on the season, but it was within approximately $\pm 1\,\mu$atm in the IrB and IcB throughout the year. In the EGC, the shift was slightly larger but still within $\pm 2\,\mu$atm throughout the year. In the NS the shift was less than $\pm 2\,\mu$atm in all months except June and July when the $d_{AS}\ fCO_2^{sw}$ estimates were decreased by 4.6 and 3.1 μatm respectively. The effect of changing to the $k-U_{10}$ parameterisation of Nightingale et al. (2000) was slightly larger, in particular for the summer months when the $d_{AS}\ fCO_2^{sw}$ estimates were reduced by up to 3 μatm in the IrB and IcB, and 5 μatm in the ECG and NS. The estimated effect of mixing plus biology changed accordingly. Still, these effects do not change the inferences drawn from Fig. 6 as they were barely discernible. As regards wind speed data, the NCEP/NCAR data appears to be too weak (Smith et al., 2001; Olsen et al., 2005; Raynaud et al., 2006). In particular, Olsen et al. (2005) showed that when calculated using QuikSCAT rather than NCEP/NCAR windspeeds, the changes in k are comparable, in absolute magnitude, to that of changing from the Wanninkhof (1992) parameterisation to that of Wanninkhof and McGillis (1999). As shown earlier this effect is insignificant for our purposes.

Finally, errors in the MLD enter directly into the $d_{AS}\ fCO_2^{sw}$ estimates. Evaluating the error in MLD is not easy due to lack of validation data. However, data from 25 XBT casts from *Nuka* in 2005 indicates that the FOAM MLD data are around 20% too deep on average. Through Eq. (A5), this translates into a potential offset in the $d_{AS}\ fCO_2^{sw}$ estimates of 20% too low, ranging from $\sim 0\,\mu$atm in winter to 3 μatm in summer in the IrB and IcB and from 0 μatm in winter up to 6 μatm in summer in the EGC and NS. The $d_{MB}\ fCO_2^{sw}$ estimates changed accordingly, but the effect was barely discernible in Fig 6.

Acknowledgements. This is a contribution to the projects A-CARB (178167/S30) and CARBON-HEAT (185093/S30) of the Norwegian Research Council, RESCUE of the Swedish National Space Board (96/05) and the EU IP CARBOOCEAN (5111176-2). This work would not have been possible without the generosity and help of Royal Arctic Lines and the captains and crew of *Nuka Arctica*. We are grateful to G. Reverdin at LOCEAN/IPSL, Paris, for generously providing the salinity and XBT data from *Nuka* for comparison with the ocean analysis data, C. Lui at the Environmental Systems Science Centre of the U.K. National Environmental Research Council for providing the FOAM data, and H. M. Jørgensen at NaviCom Marine in Denmark for his regular checks and work with the fCO_2 instrument on *Nuka*. We thank R. Bellerby and A. Omar at the Bjerknes Centre for Climate Research for their initial work in setting up an fCO_2^{sw} instrument aboard *Nuka*. We also thank H. Lüger, two anonymous reviewers and Associate Editor J. Orr for their comments that helped improve this manuscript. This is contribution # A183 of the Bjerknes Centre for Climate Research.

Edited by: J. Orr

References

Bellerby, R. G. J., Olsen, A., Furevik, T., and Anderson, L. G.: Response of the surface ocean CO_2 system in the Nordic Seas and northern North Atlantic to climate change, in The Nordic Seas: An Integrated Perspective, edited by: Drange, H., Dokken, T., Furevik, T., Gerdes, R., and Berger, W., Geophys. Monogr. Ser., 158, 189–197, AGU, Washington D.C., 2005.

Boutin, J., Etcheto, J., Dandonneau, Y., Bakker, D. C. E., Feely, R. A., Inoue, H. Y., Ishii, M., Ling, R. D., Nightingale, P. D., Metzl, N., and Wanninkhof, R.: Satellite sea surface temperature: A powerful tool for interpreting in situ pCO_2 in the equatorial Pacific Ocean, Tellus B, 51, 490–508, 1999.

Chierici, M., Fransson, A., and Nojiri, Y.: Biogeochemical processes as drivers of surface fCO_2 in contrasting provinces in the North Pacific Ocean, Global Biogeochem. Cy., 20, GB1009, doi:10.1029/2004GB002356, 2006.

Cooper, D. J., Watson, A. J., and Ling, R. D.: Variation of pCO_2 along a North Atlantic shipping route (U.K. to the Caribbean): A year of automated observations, Mar. Chem., 72, 151–169, 1998.

Corbiere, A., Metzl, N., Reverdin, G., Brunet, C., and Takahashi, T.: Interannual and decadal variability of the oceanic carbon sink in the North Atlantic subpolar gyre, Tellus B, 59, 168–178, 2007.

Cosca, C. E., Feely, R. A., Boutin, J., Etcheto, J., McPhaden, M. J., Chavez, F. P., and Strutton, P. G.: Seasonal and interannual CO_2 fluxes for the central and eastern equatorial Pacific Ocean as determined from fCO_2-SST relationships, J. Geophys. Res., 108, 3278, doi:10.1029/2000JC000677, 2003.

Feely, R. A., Wanninkhof, R., Milburn, H. B., Cosca, C. E., Stapp, M., and Murphy, P. P.: A new automated underway system for making high precision pCO_2 measurements onboard research ships, Anal. Chim. Acta, 377, 185–191, 1998.

Frantantoni, D. M.: North Atlantic surface circulation during the 1990's observed with satellite-tracked drifters, J. Geophys. Res., 106, 22 067–22 093, 2001.

Gruber, N., Sarmiento, J. L., and Stocker, T. F.: An improved method for detecting anthropogenic CO_2 in the oceans, Global Biogeochem. Cy., 10, 809–837, 1996.

Hansen, B. and Østerhus, S.: North Atlantic-Nordic Seas exchanges, Prog. Oceanogr., 45, 109–208, 2000.

Holliday, N. P., Waniek, J. J., Davidson, R., Wilson, D., Brown, L., Sanders, R., Pollard, R. T., and Allen, J. T.: Large-scale physical controls on phytoplankton growth in the Irminger Sea Part I: Hydrographic zones, mixing and stratification, J. Mar. Syst., 59, 201–218, 2006.

Kalnay, E., Kanamitsu, M., Kistler, R., Collins, W., Deaven, D., Gandin, L., Iredell, M., Saha, S., White, G., Woollen, J., Zhu, Y., Chelliah, M., Ebisuzaki, W., Higgins, W., Janowiak, J., Mo, K. C., Ropelewski, C., Leetmaa, A., Reynolds, R., and Jenne, R.: The NCEP/NCAR Reanalysis Project, B. Am. Meteorol. Soc., 77, 437–471, 1996.

Lacan, F. and Jeandel, C.: Subpolar Mode Water formation traced by neodynium isotopic composition, Geophys. Res. Lett., 31, L14306, doi:10.1029/2004GL019747, 2004.

Lee, A. J.: North Sea: Physical Oceanography, in: The North-West European shelf seas: the seabed and the sea in motion, part II physical and chemical oceanography and chemical resources, edited by: Banner, F. T., Collins, M. B., and Massie, K. S., Elsevier Oceanography Series, 24b, 467–493, 1980.

Lee, K., Tong, L. T., Millero, F. J., Sabine, C. L., Dickson, A. G., Goyet, C., Park, G.-H., Wanninkhof, R., Feely, R. A., and Key, R. M.: Global relationships of total alkalinity with salinity and temperature in surface waters of the world's oceans, Geophys. Res. Lett., 33, L19605, doi:10.1029/2006GL027207, 2006.

Lèvy, M., Lehan, Y., Andrè, J.-M., Mèmery, L., Loisel, H., and Heifetz, E.: Production regimes in the northeast Atlantic: A study based on Sea-viewing Wide Field of view Sensor (SeaWiFS) chlorophyll and ocean general circulation model mixed layer depth, J. Geophys. Res., 110, C07S10, doi:10.1029/2004JC002771, 2005.

Lueker, T. J., Dickson, A. G., and Keeling, C. D.: Ocean pCO_2 calculated from dissolved inorganic carbon, alkalinity and equations for K_1 and K_2: validation based on laboratory measurements of CO_2 in gas and seawater at equilibrium, Mar. Chem., 70, 105–119, 2000.

Lüger, H., Wallace, D. W. R., Körtzinger, A., and Nojiri, Y.: The pCO_2 variability in the midlatitude North Atlantic Ocean during a full annual cycle, Global Biogeochem. Cy., 18, GB3023, doi:10.1029/2003GB002200, 2004.

McCartney, M. S. and Talley, L. D.: The Subpolar Mode Waters of the North Atlantic Ocean, J. Phys. Oceanogr., 12, 1169–1188, 1982.

McClain, C. R., Feldmann, G. C., and Hooker, S. B.: An overview of the SeaWiFS project and strategies for producing climate research quality global ocean bio-optical time series, Deep-Sea Res. II, 51, 5–42, 2004.

McCulloch, M. E., Alves, J. O. S., and Bell, M. J.: Modelling shallow mixed layers in the northeast Atlantic, J. Mar. Syst., 52, 107–119, 2004.

Mehrbach, C., Culberson, C. H., Hawley, J. E., and Pytkowicz, R. M.: Measurement of apparent dissociation contants of carbonic acid in seawater at atmospheric pressure, Limnol. Oceanogr., 18, 533–541, 1973.

Nakaoa, S. I., Aoki, A., Nakazawa, T., Hashida, G., Morimoto, S., Yamanouchi, T., and Yoshikawa-Inoue, H.: Temporal and spatial variations of the oceanic pCO_2 and air- sea CO_2 flux in the Greenland Sea and Barents Sea, Tellus B, 58, 148–161, 2006.

Nelson, N. B., Bates, N. R., Siegel, D. A., and Michaels, A. F.: Spatial variability of the CO_2 sink in the Sargasso Sea, Deep-Sea Res. II, 48, 1801–1821, 2001.

Nightingale, P. D., Malin, G., Law, C. S., Watson, A. J., Liss, P. D., Liddicoat, M. I., Boutin, J., and Upstill-Goddard, R. C.: In situ evaluation of air-sea gas exchange parameterizations using novel conservative and volatile tracers, Global Biogeochem. Cy., 14, 373–387, 2000

Olsen, A., Wanninkhof, R., Triñanes, J., and Johannessen, T.: The effect of wind speed products and wind speed-gas exchange relationships on interannual variability of the air-sea CO_2 gas transfer velocity, Tellus B, 57, 95–106, 2005.

Olsen, A., Triñanes, J. A., and Wanninkhof, R.: Sea-air flux of CO_2 in the Caribbean Sea estimated using in situ and remote sensing data, Remote Sens. Environ., 89, 309–325, 2004.

Olsen, A., Bellerby, R. G. J., Johannessen, T., Omar, A. M., and Skjelvan, I.: Interannual variability in the wintertime air-sea flux of carbon dioxide in the northern North Atlantic, 1981–2003, Deep-Sea Res. I, 50, 1323–1338, 2003.

Orvik, K. A. and Niiler, P.: Major pathways of Atlantic water in the northern North Atlantic and Nordic Seas toward Arctic, Geophys. Res. Lett., 29(19), 1896, doi:10.1029/2002GL015002, 2002.

Park, G. H., Lee, K., Wanninkhof, R., Feely, R. A.: Empirical temperature-based estimates of variability in the oceanic uptake of CO_2 over the past two decades, J. Geophys. Res, 111(C7), C07S07, doi:10.1029/2005JC003090, 2006.

Pèrez, F. F., Àlvarez, M., and Rios, A. F.: Improvements on the back-calculation technique for estimating anthropogenic CO_2, Deep-Sea Res. I, 49, 859–875, 2002.

Pollard, R. T., Read, J. F., Holiday, N. P., and Leach, H.: Water Masses and circulation pathways through the Iceland Basin during Vivaldi 1996, J. Geophys. Res., 109, C04004, doi:10.1029/2003JC002067, 2004.

Prentice, I. C., Farquhar, G. D., Fasham, M. J. R., Goulden, M. L., Heimann, M., Jaramillo, J., Kheshgi, H. S., Le Quèrè, C., Scholes, R., and Wallace, D. W. R.: The Carbon Cycle and Atmospheric Carbon Dioxide, in Climate Change 2001: The Scientific

Basis, Contribution of Working Group I to the Third Assessment Report of the intergovernmental Panel on Climate Change, edited by: Houghton, J. T., Ding, Y., Griggs, D. J., Noguer, M., van der Linden, P. J., Dai, X., Maskell, K., and Johnson, C. A., Cambridge University Press, Cambridge, United Kingdom and New York, NY, USA, 881 pp., 2001.

Raynaud, S., Orr, J. C., Aumont, O., Rodgers, K. B., and Yiou, P.: Interannual-to-decadal variability of North Atlantic air-sea CO_2 fluxes, Ocean Sci., 2, 43–60, 2006, http://www.ocean-sci.net/2/43/2006/.

Reverdin, G., Niiler, P. P., and Valdimirsson, H.: North Atlantic Surface Currents, J. Geophys. Res., 108(C1), 3002, doi:10.1029/2001JC001020, 2003.

Roy, R. N., Roy, L. N., Vogel, K. M., Moore, C. P., Pearson, T., Good, C. E., Millero, F. J., and Campbell, D. M.: Determination of the ionization constants of carbonic acid in seawater, Mar. Chem., 44, 249–268, 1993.

Smith, S. R., Legler, D. M., and Verzone, K. V.: Quantifying uncertainties in NCEP reanalyses using high-quality research vessel observations, J. Climate, 14, 4062–4072, 2001.

Stephens, M. P., Samuels, G., Olson, D. B., Fine, R. A., and Takahashi, T.: Sea-air flux of CO_2 in the North Pacific using shipboard and satellite data, J. Geophys. Res., 100, 13 571–13 583, 1995.

Sverdrup, H. U.: On conditions for the vernal blooming of phytoplankton, J. Conc. Int. P. Exp. de la Mer, 18, 287–295, 1953.

Sweeney, C., Takahashi, T., and Gnanadesikan, A.: Spatial and temporal variability of surface water pCO_2 and sampling strategies, in: A large-scale CO_2 observing plan: In situ oceans and atmosphere, edited by: Bender, M., Doney, S., Feely, R. A., et al., National Technical Information Service, Springfield, Virginia, USA, 155–175, 2002.

Takahashi, T., Sutherland, S. C., Sweeney, C., Poisson, A., Metzel, N., Tilbrook, B., Bates, N., Wanninkhof, R., Feely, R. A., Sabine, C., Olafsson, J., and Nojiri,Y.: Global sea- air CO_2 flux based on climatological ocean pCO_2 and seasonal biological and temperature effects, Deep-Sea Res. II, 49, 1601–1622, 2002.

Takahashi, T., Olafsson, J., Goddard, J. G., Chipman, D. W., and Sutherland, S. C.: Seasonal variation of CO_2 and nutrients in the high-latitude surface oceans: a comparative study, Global Biogeochem. Cy., 7, 843–878, 1993.

Taylor, A. H., Watson, A. J., Ainsworth, M., Robertson, J. E., and Turner, D. R.: A modelling investigation of the role of phytoplankton in the balance of carbon at the surface, Global Biogeochem. Cy., 5, 151–171, 1991.

Wallace, D. W. R.: Storage and transport of excess CO_2 in the oceans: The JGOFS/WOCE global CO_2 survey, in: Ocean Circulation and Climate: Observing and Modelling the Global Ocean, edited by: Siedler, G., Church, J., and Gould, J., Elsevier, New York, 489–521, 2001.

Wanninkhof, R., Olsen, A., and Triñanes, J.: Air-sea CO_2 fluxes in the Caribbean Sea from 2002–2004, J. Mar. Syst., 66, 272–284, 2007.

Wanninkhof, R., Lewis, E., Feely, R. A., and Millero, F. J.: The optimal carbonate dissociation constants for determining surface water pCO_2 from alkalinity and total inorganic carbon, Mar. Chem., 65, 291–301, 1999.

Wanninkhof, R. and McGillis, W. R.: A cubic relationship between air-sea CO_2 exchange and wind speed, Geophys. Res. Lett., 26(13), 1889–1892, 1999.

Wanninkhof, R. and Thoning, K.: Measurement of fugacity of CO_2 in surface water using continuous and discrete sampling methods, Mar. Chem., 44, 189–201, 1993.

Wanninkhof, R.: Relationship Between Wind Speed and Gas Exchange Over the Ocean, J. Geophys. Res., 97, 7373–7382, 1992.

Watson, A. J., Robinson, C., Robertson, J. E., Williams, P. J. le B., and Fasham, M. J. R.: Spatial variability in the sink for atmospheric carbon dioxide in the North Atlantic, Nature, 350, 50–53, 1991.

Weiss, R. F.: Carbon dioxide in water and seawater: The solubility of a nonideal gas, Mar. Chem., 2, 201–215, 1974.

Weiss, R. and Price, B. A.: Nitrous oxide solubility in water and seawater, Mar. Chem., 8, 347–359, 1980.

Zeebe, R. and Wolf-Gladrov, D.: CO_2 in seawater: equilibrium, kinetics, isotopes, Elsevier Oceanography Series 65, Elsevier, Amsterdam, 346 pp., 2001.